SHIELDING DESIGN FOR THE LCLS BTH AND UNDULATOR

M. Santana Leitner, A. Fassò, T. Sanami, S. Mao, J. Liu and S. Rokni

Stanford Linear Acceleration Center: 2575 Sand Hill Road, Menlo Park, CA, 94025, msantana@slac.stanford.edu

The Linac Coherent Light Source (LCLS), the world's first hard x- ray free electron laser is under construction at the Stanford Linear Accelerator Center and is expected to be completed in 2009. LCLS will deliver unprecedented bright and short x-ray laser pulses that shall enable frontier new science research in biology, nanomaterials and non-crystalline imaging. Over 400 m of LCLS tunnel have been implemented with the Monte Carlo cascade codes Fluka and MARS15. An extensive survey has been conducted to determine the radiation levels and shielding requirements from the Beam Transfer Hall to the Near Experimental Hall, covering in detail the 33 segments of the undulator, collimators, magnets, beam lines, mirrors, hutches, etc. and considering several radiation sources.

I. INTRODUCTION

While this article is written, the LCLS tunnels and walls are steadily being poured in the east area of SLAC, following, among others, recommendations and restrictions from the Radiation Physics group at SLAC.

Broad expertise and reliable analytic tools are world-wide available for the design of lateral shieldings, but as pioneer in its kind, LCLS also challenges radiation protection with the occupancy of areas at zero-degree orientation. This happens because the electron beam (5 kW, 120 Hz, 17 GeV) is bended down (by the BYD dipole magnets) into an underground beam dump (MDUMP), while the Free Electron Laser (FEL) generated at the undulator (UND) follows the tangent straight line into the experimental hutches, together with the bremsstrahlung photon flux bred from halo-machine interceptions or beam -instrument interactions. The latter component cannot be detached of the useful light by means of magnetic fields (photons), and therefore is transported through the laser clearance of the walls towards the experimental areas, becoming a potential 'behind-the-shield' radiation source, which typically blows up in tight collimators or in X-FEL mirrors.

A second, though not less severe consequence of the 'zero-degree' shielding configuration is the fact that intense and highly forward-peaked fluxes of muons are created by the high energy electron beam. Muons are pair-produced from bremsstrahlung photons (γ, $\mu^-\mu^+$) and also proceed from the decay of photopions. Even thick walls of heavy-Z materials can barely reduce the muon doses.

In order to cope with the above mentioned challenges, extensive efforts have been dedicated to analyze the sources of radiation and to compute the necessary shieldings. Two state of the art, high energy, multi-particle transport codes, Fluka and MARS15, have been used in parallel to obtain reliable results for the key sources, while for less relevant items, either of them has been used. The methodologies have been presented to external peer-review boards composed of renowned Monte-Carlo experts, and advice has been sought at regular in-house radiation safety committees.

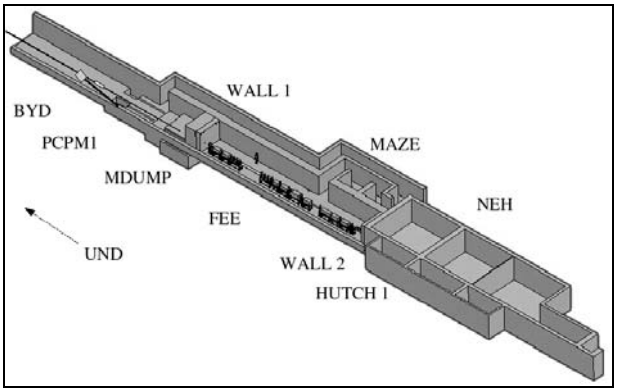

Fig. 1. Schematic 3D view for the LCLS between the electron dump hall and the NEH. The undulator and BTH are upstream.

I.A. Geometry and sources

This article covers the part of LCLS accelerator comprised between the end (Z=387) of the DL2 momentum cleaning insertion at Beam Transfer Hall (BTH) and the Near Experimental Hall (NEH), (Z=790 m).

DL2 includes a set of short two-jawed tungsten secondary x-y halo cleaning collimators (CX/Y31-38) and a tune-up dump (TDUND), which should withstand the dumping of the electron beam at 30 Hz (420 W).

Next, the electron beam goes through the *undulator* (UND), which is a structure of 11 periods, each of which has three equispaced wigglers (called segments) with quadrupole magnets in between. The 33 segments, arranged in series, contain a periodical structure of 226 poles/magnets, which allow the powerful LCLS laser light to be build up from the coherent interference between the electron beam and the synchrotron light that is created in the small kicks induced by the magnets.

The photon and the electron beams travel together until the *beam dump hall* (BHALL). In this zone the BYD deflects the electrons to MDUMP while the photon beam keeps straight. Radiation losses in BYD are locally shielded with several iron slabs (PCPM1 and PCPM2) that have small clearance holes for the photon line. In case of power failure of BYD, the electron beam would be pointing towards the downstream experimental areas. This accident scenario is mitigated with an additional (horizontal)-dipole made of permanent magnet material, which would send the electron beam sideward into a safety dump (SDUMP).

When personnel is working in the Front End Enclosure (FEE), three beam stoppers (ST1-3) are inserted to intercept the laser and the bremsstrahlung beams, as well as the radiation that would stream through the photon beam pipe.

Wall 1 separates the beam dump hall from the FEE, where eventually personnel will be present to fix settings for laser physics. This wall has 16 iron plates of a total thickness of 1.22 m (4'), followed by 0.91 m (3') of concrete. The photon beam pipe through the wall has a diameter of 9.53 cm (3.75"). Numerous simulations were performed for different arrangements and designs of the iron plates. In particular, it was found that the small gaps (of the order of 10 cm) left around the perimeter of the massive iron plates ought to be filled with concrete or with a grout aggregate that would include iron.

The (FEE) is a 35 m long section comprised between Wall 1 and Wall 2 (described later). The photon line in the FEE goes through several concentric collimators and it is horizontally split by mirrors into one high energy line (HEL) and two low energy lines (LEL) that form 60 and 90 mradian with respect to the HEL. The HEL is kicked 3.264 cm sideward by two mirrors. A faint, yet noxious, bremsstrahlung flux makes it through Wall 2 into the NEH and may give way to a radiation source when interacting with valves, collimators or other equipment pieces. First calculations show that most of this radiation can be absorbed by having a lead shielded pipe. This paper is devoted to construction phase I, where pipes are not yet installed in the NEH. Thus, all the three lines will be locked before Wall 2 by a set of two stoppers called hutch shutters (SH).

The FEE and the experimental hutch 1 of the NEH are separated by Wall 2. The design of Wall 2 is almost identical to that of Wall 1 with a few exceptions, the main ones being the integrated thickness of the iron plates (92 instead of 122 cm) and the number of beam pipe holes (three instead of one).

In summary, the sequence of key sections (and components), as abbreviated in this note is: BTH, UND, BHALL (BYD, SDUMP, MDUMP), (WALL1), FEE, (WALL2) and NEH.

Further information about the materials and sizes of all the objects involved in the simulations can be found in (Ref. 1).

I.B. Sources of radiation

The main goal of these studies is the accurate determination and minimization of the peak dose rate equivalent in the infrequently occupied FEE (limit established at 5 μSv/h) and in the experimental area NEH (limit is 0.5 μSv/h).

In general terms, the radiation in these zones is either carried by muons directly from the beam loss spots, or indirectly through bremsstrahlung photon beams, which ultimately scatter in beam instrumentation and originate secondary sources in the vicinity of the surveyed zones. A third relevant component is that of high energy neutrons, moderated in the hydrogenated media (concrete).

The loss spots and conditions (rather pessimistic) have been defined as follows (Ref. 2): Up to 20 W of electrons *lost* in the collimators of BTH (1), 420 W in TDUND (2), 20 W in BYD (3) and 5000 W in MDUMP (4). Moreover, the 5000 W carried by the beam may be *intercepted* (5) by the beam finder wires (BFW). Note that *2* is only compatible with *1*. The other four sources may be present simultaneously.

I.C. Computational tools and techniques

The latest version of Fluka (Ref. 3, 4) Monte Carlo multi particle transport code has been used (2006.3b), with a broad set of user-written routines. All the geometry described above has been carefully described. *Lattice* capabilities have been enabled in order to replicate several complex objects (i.e. Segments, quadrupoles, stoppers and collimators) from a single prototype implementation. In this regard, and following the technique used earlier at (Ref. 5), a script has been developed to automatically retrieve the newest object locations from the *beam optic files* (Ref. 6) and to write them into the Fluka input file.

The call to the Fluka magnetic field routine has been activated, and the routine has been customized to include the fields in segments, dipoles (including yoke) and quadrupoles. Moreover, a special routine was written to accept mirror-like reflections of photons grazing the smoothly polished aluminum inner surface of the beam pipe with angles shallower than the critical angle defined in equation 1.

$$\theta_{crit}[rad] = \frac{3.162 \cdot 10^{-8}}{E_\gamma [GeV]} \qquad (1)$$

Many preprocessor instructions were set so that all sources, geometrical configurations, physics models, etc. would coexist in harmony within a single input file. This ensures that all cases benefit equally of upgrades in geometry, etc. and it avoids versions to diverge with changes.

The energy density to dose equivalent transformation was carried out by using the scoring functions (Ref. 7, 8). As for the bremsstrahlung calculations, the online scoring routine was adapted and, in addition, existing post-processing programs were linked and extended by newer ones.

In addition, MARS15 Monte Carlo code (Ref. 9-12) also used to cover sources 3 and 4, as well as for other calculations that escape the scope of this note. Thus, the MARS geometry file covers the BHALL-NEH section (not BTH-UND), with greater detail around MDUMP and including also the side mazes and the upper ground landscape.

I.D. Scheme of the calculations

Initially, simplified Fluka calculations with basic loss assumptions were performed to estimate the bulk shielding requirements of Wall 1 and Wall 2 (Ref. 13).

Next, a more realistic geometry was implemented in two sections. The first part focused on Wall 1 design and spanned from BTH to FEE (Ref. 1, 14). The second part, for Wall 2 design, included the FEE and the NEH (Ref. 14, 15). The parallelization of the tasks allowed sharing the work to provide second-order estimations in a timely manner. In order to decouple the FEE-NEH section from the upstream sources, the contribution to the dose in NEH from muons born before Wall 1 was neglected, while the dose from bremsstrahlung interactions was tentatively simulated by intercepting a 2kW beam with a 14 micron Ti foil. This would produce a photon power of 800 mW, which would induce peak doses in the NEH five times above the limit of 0.5 μSv/h. The doses obtained in NEH (part II) were normalized to the bremsstrahlung powers obtained in the BTH-FEE section (part I) as soon as those were being obtained.

The input files for the two sections were written with compatible formats, in absolute coordinates and with a common reference frame. This eased the final assembly of the two geometry descriptions into a single one, once those were mature and fully debugged. Thus, in the third step, estimations were refined by having radiation fully transported from all sources down to both FEE and NEH.

Results from BYD and MDUMP sources were also computed with MARS15 code (Ref 16, 17).

This article refers to the last set of calculations (full model).

II. RESULTS

The first two subsections explain the contribution to the dose in NEH and FEE from each loss source, including the permanent (normal operation) and temporary sources (insertions). The last subsection collects the different terms for several operation regimes. The total loss should stay below 5 μSv/h in FEE and 0.5 μSv/h in NEH.

II.A. Sources for continuous losses

Among the five loss spots introduced in section I.A. three sources may contribute to radiation levels continuously: the collimators, C{X/Y}31-38, the BYD magnet and the main dump, MDUMP.

II.A.1. Doses induced by 20 W losses in CY38

The C{X/Y} is a sequence of six vertical (Y) and horizontal (X) collimators designed to remove some secondary halo and dark current effects. If C{X/Y}31-38 had been energy or position cleaning collimators, the *momenta* and coordinates of the particles removed from the halo could have been determined with certain precision, but in this case neither the 6-coordinate, nor the total removed power are precisely known.

In normal operation it is expected that the losses will not surpass 1 W, but the maximum credible loss has been set at 20 W. As for the position and momentum of the intercepted electrons, spatial uniformity was assumed, while preliminary simulations scanned the importance of the grazing angle (1 and 0.1 mradian). The shallower angle was retained for simulations because it provided conservative results and it was still believed to be compatible with the roughness of the collimator surface.

The 20 W were deposited in the last collimator. Fine tuning of this hypothesis could have been carried out; however, the effort was not considered a priority, as the results shown in Table I prove that this source is rather weak. This fact is explained by the relative low intensity of the source and its large distance to the FEE (227 m) and NEH (263 m).

The grazing beam at CY38 produces showers from the collimator all the way down to the FEE wall, inducing doses of 10 mSv/h at the end of the undulator. This flux is readily stopped by the bulk shielding of Wall 1. The second component of radiation is the bremsstrahlung flux created at the jaws of the collimator. If the ST1-3 stoppers are out, photons can go through Wall 1 hole and reach the FEE with a power of about 15 mW. The subsequent showers in mirrors and collimators give rise to doses in FEE of up to 10 mSv/h. Wall 2 stops these cascades from

reaching the NEH. Thus, in normal operation (CY38 source could exist continuously) NEH is protected but FEE can only be occupied if the ST1-3 stoppers are inserted. By doing so, the 15 mW photon flux is stopped and the FEE is well protected.

TABLE I. Peak doses in FEE and NEH [μSv/h] for several loss components and combinations of them. Accepted limits are 5 and 0.5 μSv/h, respectively. Totals are not direct sums of individual contributions (*) means 30 Hz instead of 120. TOT sums explained in sec. II.C

Mode	TDUND	IN		OUT		
	ST	IN or OUT		IN		OUT
Loss	Source	FEE	NEH	FEE	NEH	NEH
20	CY38	*0*	*0*	*5E-3*	*1E-4*	*0.03*
420*	TDUND	*0.5*	*0.1*	-	-	-
20	BYD	-	-	*2.0*	*0.1*	*0.05*
5000	MDUMP	-	-	*0.5*	*1E-3*	*1E-3*
	TOT-1	*0.5*	*0.1*	*2.0*	*0.1*	*0.1*
5000	BFW33	-	-	*0.2*	*0.1*	*1.5*
5000	**TOT-2**	-	-	*2.0*	*0.1*	*1.5*
1225*	**TOT-3**	*0.5*	*0.1*	*0.5*	*0.03*	*0.38*

II.A.2. Doses induced by 20 W loss in BYD

Like for the CY38 collimator, losses in BYD are marginally known. Therefore, a similar approach was followed, e.g. it has been accepted that 20 W can be lost in BYD.

An initial pessimistic yet possible assumption concentrated the losses right at the entrance of BYD on the inner surface the beam pipe and with a grazing angle of 0.1 mradian in the y-z plane. This mis-steering situation would lead to over 1.4 W of bremsstrahlung power into the FEE, thus inducing doses in NEH 4 times above the limit. A beam shut-off ion chamber is required to handle these cases.

Another less pessimistic, though still conservative scenario contemplates 20 W losses distributed along the inner pipe surface at the right side of the beam orbit, with the same grazing angle of 0.1 mradian. The bremsstrahlung photon power reaching the FEE is about 0.037 W, well below the 0.400 W limit obtained in the preliminary calculations for FEE-NEH. However a fraction of the photons that don't reach the FEE (due to the bend of the beam) create muons that partly reach the NEH. In order to evaluate the combined effect of both types of radiation, detailed simulations were run both with Fluka and MARS15.

The computed peak dose in NEH (ST OUT, SH IN) is lower than 0.05 μSv/h. The highest doses are found above the horizontal beam plane. The dose in FEE (ST IN, SH IN) is not bigger than 2 μSv/h.

II.A.3. Doses generated in the 5 kW beam dump

The main dump (MDUMP) has been designed to continuously withstand beam of up to 5 kW at 17.0 GeV, 120 Hz (Ref. 18, 19). MDUMP is buried short before Wall 1, well covered and surrounded by big metal plates. Since the beam is dumped from above with a certain angle, most of the streaming radiation points downwards behind MDUMP. Tritium production and water activation were checked in (Ref. 20).

As for the dose in the FEE and NEH, it is almost independent of the insertion of ST1-3 stoppers (indeed dose maps look identical), and amounts to 0.5 and 1E-3 μSv/h, respectively.

II.B. Temporary loss sources

The beam can be fully stopped by thick inserted objects, or it can produce a flux of bremsstrahlung photons in thin measurement objects like wire scanners or beam finder wires.

II.B.1. Doses induced by 420 W losses in TDUND

In this case the beam is *stopped* in the tune up dump at a frequency of 30 Hz, 4 times below the running value (120 Hz). This means that all powers need be scaled accordingly. Moreover, the contribution from downstream sources vanishes (stopped beam).

Simulations (Table I) show that the contribution to the peak dose of TDUND in FEE and NEH is very low. TDUND is followed by a massive concentric collimator, which provides one order of magnitude dose reduction (included). This component is not required in terms of FEE and NEH dose, but it may be important to reduce the neutron fluence in the first segments of the undulator, which otherwise may have their life shortened due to demagnetization (Ref. 21).

II.B.2. Doses induced by exposing thin objects to the 5000 W electron beam

In this case, a thin wire or a screen is temporally inserted in the central orbit of the electron beam. A significant flux of photons is then created through bremsstrahlung interactions between the electron beam and the field of the atoms of the instrument. These photons are strongly forward peaked and, therefore, they are able to follow a long fraction of the laser path, bypassing the shieldings and ultimately interacting with mirrors and photon collimators. Moreover, the electrons of the beam are slightly deviated in the interaction with

the wire, which increases the emittance and leads to additional losses.

In (Ref. 1, 11), insertions were extensively studied, including several wire materials, diameters, locations and orientations, etc. The worst possible, yet acceptable scenario results from the insertion of the closest instrument to the FEE (BFW33 is the last one).

BFW33 is limited to a diameter of 40 micron. The average thickness (<d>) crossed by the 30 micron Gaussian beam is 80% of the value. The radiation lengths (X_0) of typical insertion materials (C, Al, Ti and W) are well beyond the sensed diameter size, meaning that BFW will act as thin target. Thus, the bremsstrahlung power will be scalable to the normalized thickness, expressed in units of radiation length (<d>/X_0).

A graphite wire (X_0 = 21.5 cm) yields 0.95 W of photons, all directed towards the Wall 1 FEE inlet hole. According to the preliminary separate FEE-NEH simulations, such a value would originate doses behind NEH exceeding the allowed limit in a small region around the pipe. This means that heavier materials shouldn't be employed. For instance, tungsten (X_0 = 0.35 cm) would produce 0.95 x (21.5/0.35) = 58 W of bremsstrahlung, with the according blast of the dose.

Detailed simulations for the dose with the full geometry model confirm these predictions. With the carbon wire, the dose in NEH (stoppers out) reaches 1.5 μSv/h in the small region behind Wall 2 around the pipe. This value exceeds the established limit of 0.5 μSv/h. In order to reduce it, insertion of BFW should be interlocked to 30 Hz, so that beam power would be reduced by factor 4, and, likewise the dose, which would not exceed 0.4 μSv/h. During FEE occupancy the ST1-3 stoppers would have to be inserted, thereby blocking the bremsstrahlung trajectory (but also the laser). The peak dose in FEE at 30 Hz would be under 0.05 μSv/h (<0.025 μSv/h in NEH). In the event of an *accidental* insertion of a tungsten wire at 30 Hz, the dose in NEH for ST OUT configuration would reach 25 μSv/h, while the peak in FEE for ST IN would top at 5 μSv/h (<2.5 μSv/h in NEH).

As for the orientation of the BFW, it doesn't modify the bremsstrahlung power. However, the vertical BFW produces a larger emittance blow-up in the vertical plane, which may ultimately lead to some more losses in BYD than those with the horizontal BFW.

Wire scanners (WS) and OTR's are made of heavier (Al and Ti) material, but they are thinner (20 and 1 micron) and are placed very far from Wall 1.

II.C. Global dose rate peaks

Table I summarizes the contributions to the dose of each source. The results are aligned in columns for three major cases: (1) TDUND inserted, (2) TDUND not inserted and ST inserted or (3) TDUND not inserted and ST inserted. In any case SH (hutch shutters) are inserted (Phase I). Every case, except for the third, displays two columns, one for the dose in FEE and another for the dose in NEH. The global dose in presence of all continuous sources and of those from TDUND appears in the row TOT-1. TOT-2 shows the peak when *BFW33* is *additionally* inserted at 120 Hz, while TOT-3 reflects the same case at 30 Hz.

Note that the totals are not a direct sum of the contributing peaks. The surveyed areas (FEE and NEH) are very large and not all the sources are aligned (e.g. MDUMP and BYD). Thus, the dose patterns differ, and the absolute peak can be anywhere between the highest maximum and the sum of all the maxima. In order to evaluate the absolute maximum, a program was written to perform a (loss) weighted sum of the different dose maps.

III. CONCLUSIONS AND OUTLOOK

Zero-degree shielding design for FEE and NEH zones required using a broad fan of techniques and intensive use of Monte Carlo transport codes, namely Fluka and MARS15. In order to speed up and obtain first-order guidelines, the geometry was initially split in two regions and two-step assumptions allowed the coupling.
A fully integrated simulation with the entire geometric description refined the initial results.

Those show that among the five identified loss sources, the two most remote ones (upstream collimators and tune-up dump) almost don't contribute to the dose in the occupied areas.

According to simulations, the insertion of beam finder wires close to FEE must be interlocked to a reduction of the beam frequency to 30 Hz. Moreover, materials heavier than graphite should be banned as insertion instruments. In any case, access to the FEE shall not be granted while the ST stoppers are out.
The losses in BYD and the dumping of the beam in MDUMP are the main continuous contributors to the dose in FEE and NEH.

Unless all credible losses happen in a single point at the entrance of BYD and with very shallow angles (mis-steering), the peak doses in FEE and NEH are comfortably below the allowed limits. Otherwise beam shut-off ion chambers will close down the beam.

ACKNOWLEDGMENTS

This work was supported by Department of Energy contract DE-AC02-76SF00515

REFERENCES

1. M. SANTANA LEITNER et. Al., "Prompt dose study in the LCLS undulator", *SLAC Radiation Physics Note* **RP-07-05**, (2007).
2. D. DOWELL, P. EMMA, J. WELCH, "Electron Beam Loss in the LCLS", *LCLS Physics Requirement Document*, 1.1-011, SLAC (2006).
3. A. FASSO, A. FERRARI and P.R. SALA, "Electron-Photon Transport in Fluka: Status," *Proc. Monte Carlo 2000 Conference*, Lisbon, October 23--26 2000, A. Kling, F. Barao, M. Nakagawa, L. Tavora and P. Vaz eds., Springer-Verlag Berlin, pp. 159–164 (2001).
4. A. FASSÒ, A. FERRARI, J. RANFT and P.R. SALA, "Fluka: Status and Prospective for Hadronic Applications", same proceedings, pp. 955–960 (2001).
5. V. VLACHOUDIS, A. FERRARI, M. MAGISTRIS, M. SANTANA LEITNER and K. TSOLOU, "Energy Deposition Studies for the Betatron Cleaning Insertion", *Particle Accelerator Conference 2005 proceedings, Knoxville, Tennessee (2005).*
6. P. EMMA, *LCLS Linac Current Beaml-line Design Optics Files*, www-ssrl.slac.stanford.edu/lcls/linac/optics
7. S. ROESLER and G.R. STEVENSON, "deq99.f - A Fluka user-routine converting fluence into effective dose and ambient dose equivalent", *Technical Note* CERN-SC-2006-070-RP-TN, EDMS No. 809389, CERN (2006).
8. M. PELLICCIONI, "Overview of fluence-to-effective dose and fluence-to-ambient dose equivalent conversion coefficients for high energy radiation calculated using the Fluka code", *Radiation Protection Dosimetry*, **88**, pp. 279–297 (2000).
9. N.V. MOKHOV, "The Mars Code System User's Guide", Fermilab-FN-628 (1995).
10. O.E. KRIVOSHEEV, N.V. MOKHOV, "MARS Code Status", Proc. Monte Carlo 2000 Conf., pp. 943, Lisbon, October 23-26, 2000; Fermilab-Conf-00/181 (2000).
11. N.V. MOKHOV, "Status of MARS Code", Fermilab-Conf-03/053 (2003).
12. N.V. MOKHOV, K.K. GUDIMA, C.C. JAMES et al, "Recent Enhancements to the MARS15 Code", Fermilab-Conf-04/053 (2004).
13. M. SANTANA LEITNER, A. FASSÒ, "Studies on Bremsstrahlung sources in the LCLS undulator", *SLAC Radiation Physics Note* **RP-07-04** (2007).
14. FASSÒ, J.C. LIU and X.S. MAO, "Shielding Design for the LCLS Front End Enclosure," *Radiation Physics Note*, **RP-07-06,** SLAC (2007).
15. A. FASSÒ and J.C. LIU, "Shielding Design for the LCLS Near Experimental Hall," *Radiation Physics Note,* **RP-07-11**, SLAC (2007).
16. T. SANAMI and X.S. MAO, "Prompt Dose in Front-end-enclosure of the LCLS facility for beam losses at BYD, ST1 and Safety dump," *Radiation Physics Note,* **RP-07-01,** SLAC (2007).
17. T. SANAMI and X.S. MAO, "Safety analysis for safety dump line of the LCLS facility", Radiation Physics Note, RP-07-03, SLAC (2007).
18. D.R. WALZ, A. McFARLANE and E. LEWANDOWSKI, "Beam Dumps, Stoppers and Faraday Cups at the SLC", *SLAC-Pub-49*, p. 2, April 1989 (A).
19. T. SANAMI, M. SANTANA LEITNER, X.S. MAO, and W.R. NELSON, "Calculation of Energy Distribution and Instantaneous Temperature Rise for the Design of the LCLS 5 kW Electron Dump", *Radiation Physics Note,* **RP-07-16,** SLAC (2007).
20. T. SANAMI and X.S. MAO, "Shielding Design for the LCLS 5 kW Electron Beam Line", *Radiation Physics Note,* **RP-07-15,** SLAC (2006).
21. A. FASSÒ, "Dose Absorbed in LCLS Undulator Magnets," *Radiation Physics Note*, **RP-05-05**, SLAC (2005).